Computers & Fluids 114 (2015) 130–140

Contents lists available at ScienceDirect

Computers & Fluids

journal homepage: www.elsevier.com/locate/compfluid

Large eddy simulation of turbine internal cooling ducts

J. Tyacke *, P.G. Tucker

Whittle Laboratory, Department of Engineering, University of Cambridge, Cambridge, UK

ARTICLE INFO

Article history:
Received 12 June 2014
Received in revised form 24 January 2015
Accepted 27 February 2015
Available online 11 March 2015

Keywords:
LES
Turbine
Heat transfer
RANS
SGS

ABSTRACT

Large-Eddy Simulation (LES) and hybrid Reynolds-averaged Navier–Stokes–LES (RANS–LES) methods are applied to a turbine blade ribbed internal duct with a 180° bend containing 24 pairs of ribs. Flow and heat transfer predictions are compared with experimental data and found to be in agreement. The choice of LES model is found to be of minor importance as the flow is dominated by large geometric scale structures. This is in contrast to several linear and nonlinear RANS models, which display turbulence model sensitivity. For LES, the influence of inlet turbulence is also tested and has a minor impact due to the strong turbulence generated by the ribs. Large scale turbulent motions destroy any classical boundary layer reducing near wall grid requirements. The wake-type flow structure makes this and similar flows nearly Reynolds number independent, allowing a range of flows to be studied at similar cost. Hence LES is a relatively cheap method for obtaining accurate heat transfer predictions in these types of flows.

1. Introduction

In gas turbines, high pressure turbine blades operate in an environment where gas temperatures are significantly higher than the safe operating temperature of the metal. This harsh environment requires the blade to be adequately cooled to prevent premature wear or failure. Hence, to continue to make improvements in efficiency and lifespan, reliable predictive technology is of great importance. Internal cooling passages are used to reduce metal temperatures and often incorporate ribs and other intricate structures to increase turbulence and hence heat transfer within such ducts. A schematic indicating turbine blade internal cooling ducts and an idealised geometry is provided in Fig. 1. In this figure, serpentine passages (passages with 180° bends) containing ribs are visible. It is well known that such flows challenge turbulence models.

Turbulence modelling in industry is dominated by the use of RANS models, which are often poor at predicting both the flow and heat transfer in complex geometries with separated flow. For example, Ooi et al. [1] study cooling passage heat transfer using the $v^2 - f, k - \varepsilon$ and Spalart–Allmaras RANS model. Secondary flow structures are found not to be modelled well using the eddy viscosity concept. In some cases, differences between other RANS models varies by approximately 100% [2].

Saha and Acharya [3] contrast unsteady-URANS (URANS) ($k - \varepsilon$ model) and LES (Dynamic Smagorinsky model [4]) approaches to model rotating and non-rotating ribbed ducts. Tafti [5] studies a periodic ribbed duct section using quasi-DNS (quasi-Direct Numerical Simulation) and LES using the Dynamic Smagorinsky model. Both quasi-DNS and LES were found to be within 10–15% of each other and within 15–30% of experimental data dependent on mesh resolution. Sewall et al. [6] investigate flow and heat transfer in the developing, fully developed, and bend regions of a ribbed duct with a 180° bend. LES matches with mean velocity, Reynolds stresses and heat transfer measurements to within 10–15%. Viswanathan and Tafti [7] compare LES and Detached Eddy Simulation (DES) [8] (LES with an extensive near wall RANS region) in the same ribbed duct. DES was found to improve predictions over the RANS. It did not however capture shear layer transition accurately, predicting a development length around two rib pitches greater than the LES. Ramgadia and Saha [9] use LES to study a periodically repeating ribbed duct section. A shear-improved Smagorinsky model is used, with LES data agreeing with measurements.

The above has shown that relative to RANS, LES is promising. This is especially so for this type of flow. For example, the often cited limitation of LES is the extreme increase in grid count with Reynolds number ($\approx Re^{2.5}$ [10]). As noted by [11–13], ribbed passage flows are Reynolds number independent. They are governed by large scales of turbulence, of the order of the rib height. Hence, in this paper, we seek to explore the benefits of LES relative to RANS. In the above, the range of LES models evaluated and strategies considered was limited. Hence, here we seek to contrast a range of LES models. These include Numerical-LES (NLES), hybrid RANS–NLES and linear and nonlinear LES subgrid scale (SGS)

* Corresponding author.
E-mail address: jct53@cam.ac.uk (J. Tyacke).

http://dx.doi.org/10.1016/j.compfluid.2015.02.022
0045-7930/

Nomenclature

C	model constant	t	time
D	duct height	u, v, w	Cartesian velocity components, m/s
P	turbulence production	y^+	wall distance in wall units
Pr	Prandtl number	ave	average
Re	Reynolds number	i	component
T	turbulent	in	inlet
$\dot{m}$	mass flowrate, kg/s	L, α, K	Leray, α, Kosović
$\mathbf{x}$	coordinate direction	T	temperature, K
$\tilde{d}$	modified wall distance	x, ax	axial
d	wall distance	CD	central difference
h	rib height	ε	turbulence dissipation rate
k	turbulent kinetic energy		
l	length scale		

models. We also note that inflow sensitivity has not been fully explored. To this end, we bracket a measured 2% intensity with an extreme range of intensities to study this aspect.

The paper is set out as follows. The problem definition, governing equations and numerical details are presented. The turbulence modelling section then introduces the SGS and hybrid RANS–NLES models used and inflow conditions. The results section then discusses flow and turbulence statistics, in addition to heat transfer, before conclusions are drawn.

2. Problem definition

The ribbed passage studied is shown in Fig. 2 and is consistent with that of [7]. The duct, comprising of an inlet and outlet leg connected with a 180° section includes 24 pairs of ribs on the top and bottom surfaces. Every surface is maintained at an arbitrary temperature of 294 K with the inlet air temperature fixed at 274 K. The duct inlet, 180° bend and outlet legs have a cross section of $D \times D$, where D = 0.149 m. The ribs have a width × height × length of $h \times h \times D$, where $h = 0.1D$. The pitch P, between ribs as marked with dotted lines in Fig. 2, is equal to D and each pair of ribs are aligned vertically. The width of the central divider is $0.5D$. The Reynolds number $Re = 20{,}000$ is based on the bulk velocity U_0 and D. A schematic of the geometry (not to scale) is shown in Fig. 3.

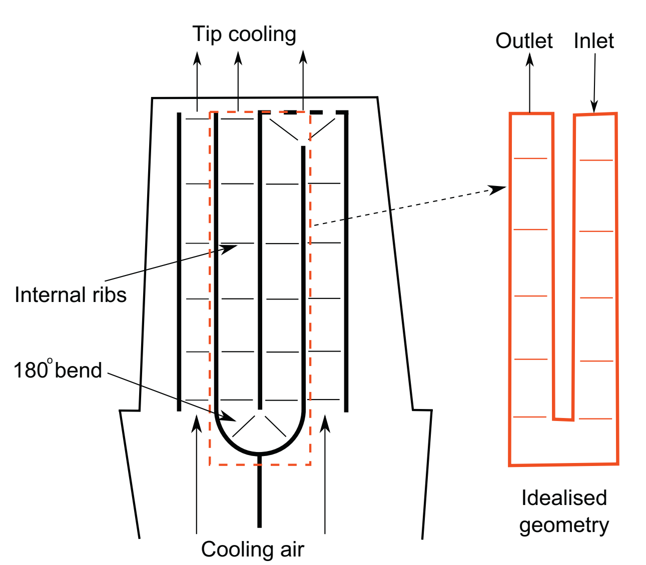

Fig. 1. Schematic showing turbine blade internal cooling ducts with rib turbulators and the idealised geometry.

3. Governing equations

The incompressible governing equations for (U) RANS/LES are based on the weakly conservative form of the Navier–Stokes equations as in Eqs. (1) and (2), the temperature equation given in Eq. (3). The tilde () symbol represents either RANS or LES variables in these equations. The key difference between typical (U) RANS and LES is the averaging in time to obtain the (U) RANS equations and spatial filtering to obtain the LES equations. Both methods are explained in detail by Pope [14]. For (U) RANS, variables are split into a time mean and mean fluctuating component. For LES, the spatial filtering results in large resolved filtered scales and sub-grid scales which are not resolved. These time-average and filtering operations (represented by the tilde symbol) give rise to the need to close the set of equations by modelling the Reynolds or subgrid scale (SGS) stress tensor respectively. This is denoted by τ_{ij} in Eq. (2). For the temperature equation, the heat flux tensor h_j is also modelled. For linear turbulence models, only the eddy viscosity μ_T requires calculation, for nonlinear models additional terms are added to τ_{ij}.

$$\frac{\partial \tilde{u}_j}{\partial x_j} = 0 \tag{1}$$

$$\rho\frac{\partial \tilde{u}_i}{\partial t} + \rho\frac{\partial(\tilde{u}_i\tilde{u}_j)}{\partial x_j} = -\frac{\partial \tilde{p}}{\partial x_i} + \frac{\partial}{\partial x_j}\left[\mu\frac{\partial \tilde{u}_i}{\partial x_j}\right] - \frac{\partial \tau_{ij}}{\partial x_j} \tag{2}$$

$$\rho\frac{\partial \widetilde{T}}{\partial t} + \rho\frac{\partial\left(\tilde{u}_j\widetilde{T}\right)}{\partial x_j} = +\frac{\partial}{\partial x_j}\left[\frac{\mu}{Pr}\frac{\partial \widetilde{T}}{\partial x_j}\right] - \frac{\partial h_j}{\partial x_j} \tag{3}$$

4. Numerical details

4.1. Solver details

The solver used is a modified version of the NEAT code as provided by Tucker [15]. This is an incompressible finite volume code

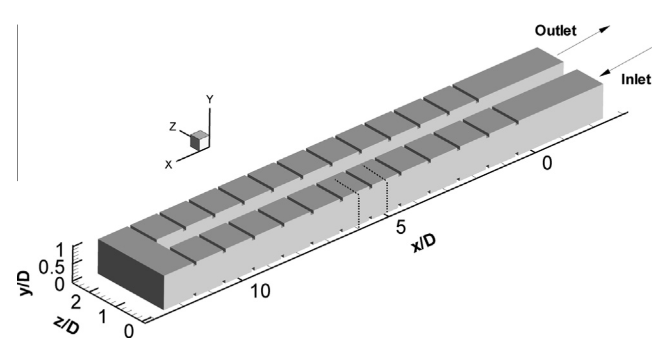

Fig. 2. Ribbed passage geometry.